

1 **Manuscript Number:**

2 **Article Summary Line:** Raccoon dogs are susceptible to and efficiently transmit SARS-CoV2

3 and may serve as intermediate host

4 **Running Title:** Susceptibility of raccoon dogs for SARS-CoV-2

5 **Keywords:** Raccoon dog, COVID-19, SARS-CoV-2, susceptibility, transmission, intermediate

6 host

7 **Title:** Susceptibility of raccoon dogs for experimental SARS-CoV-2 infection

8 Conrad M. Freuling<sup>1</sup>, Angele Breithaupt<sup>1</sup>, Thomas Müller, Julia Sehl, Anne Balkema-

9 Buschmann, Melanie Rissmann, Antonia Klein, Claudia Wylezich, Dirk Höper, Kerstin

10 Wernike, Andrea Aebischer, Donata Hoffmann, Virginia Friedrichs, Anca Dorhoi, Martin H.

11 Groschup, Martin Beer<sup>2</sup>, Thomas C. Mettenleiter<sup>2</sup>

12 **Affiliations:**

13 Friedrich-Loeffler-Institut, Greifswald-Insel Riems, Germany

14 <sup>1</sup> Authors contributed equally to this work

15 <sup>2</sup> Corresponding authors

16 Address for correspondence:

17 Martin Beer, Institute of Diagnostic Virology, Friedrich-Loeffler-Institut, Südufer 10, 17493

18 Greifswald - Insel Riems, Germany, Email: [Martin.Beer@fli.de](mailto:Martin.Beer@fli.de), Telephone: +49 38351 7-1200,

19 Fax: +49 38351 7-1226 and Thomas C. Mettenleiter, President, Friedrich-Loeffler-Institut,

20 Südufer 10, 17493 Greifswald - Insel Riems, Germany, Email: [ThomasC.Mettenleiter@fli.de](mailto:ThomasC.Mettenleiter@fli.de),  
21 Telephone: +49 38351 7-1250, Fax: +49 38351 7-1151

## 22 **Abstract**

23 Severe acute respiratory syndrome coronavirus 2 (SARS-CoV-2) emerged in China at the end of  
24 2019, and became pandemic. The zoonotic virus most likely originated from bats, but definite  
25 intermediate hosts have not yet been identified. Raccoon dogs (*Nyctereutes procyonoides*) are  
26 kept for fur production, in particular in China, and were suspected as potential intermediate host  
27 for both SARS-CoV6 and SARS-CoV2. Here we demonstrate susceptibility of raccoon dogs for  
28 SARS-CoV-2 infection after intranasal inoculation and transmission to direct contact animals.  
29 Rapid, high level virus shedding, in combination with minor clinical signs and pathohistological  
30 changes, seroconversion and absence of viral adaptation highlight the role of raccoon dogs as a  
31 potential intermediate host. The results are highly relevant for control strategies and emphasize  
32 the risk that raccoon dogs may represent a potential SARS-CoV-2 reservoir. Our results support  
33 the establishment of adequate surveillance and risk mitigation strategies for kept and wild  
34 raccoon dogs.

## 35 **Text**

36 Coronaviruses can infect a wide variety of animals, and are responsible for human  
37 diseases including severe acute respiratory syndromes (SARS). Both SARS coronavirus (SARS-  
38 CoV) (1, 2) and Middle East Respiratory Syndrome coronavirus (MERS-CoV) (3, 4), are  $\beta$ -  
39 coronaviruses and presumably originate from bats (5). They likely adapted to other reservoir  
40 hosts like Asian palm civets (*Paradoxurus hermaphroditus*) (6) and dromedary camels (*Camelus*  
41 *dromedarius*) (7). Natural SARS-CoV infections were also detected in raccoon dogs

42 (*Nyctereutes procyonoides*) which, among other candidate species, have been discussed as a  
43 possible intermediate host for the first SARS-pandemic of 2002/2003 (8).

44 The current SARS-CoV-2 pandemic started from Wuhan, China, at the end of 2019.  
45 Close relatives to SARS-CoV-2 were found in bats (9), and pangolins (*Pholidota spp*) (10, 11).  
46 Furthermore, spill-over infections to different carnivores (dogs, cats, lions, tigers and minks)  
47 were reported (12, 13). However, whether the pandemic started by a direct transmission of the  
48 SARS-CoV-2 ancestor from bats to humans or via an intermediate mammalian host with further  
49 adaptation, is still under debate (14). For both, SARS-CoV and MERS-CoV, intermediate hosts  
50 played a crucial role in transmission to humans. However, no definite intermediate host for  
51 SARS-CoV-2 has been identified up to now (14), but animal species like pangolins, palm civets,  
52 or raccoon dogs are discussed (15–17). Although the pandemic is driven by direct human-to-  
53 human transmission, case studies demonstrate that anthro-zoonotic infections occurred by  
54 contact of infected humans with companion animals and farmed minks kept for fur production in  
55 the Netherlands, Denmark and Spain (13, 18, 19). There is also evidence for zoo-anthroponotic  
56 infection of humans (13).

57 Natural infections of raccoon dogs with SARS-CoV were reported (8), indicating a  
58 potential role in the previous SARS-CoV epidemic. In fact, 14.14 million captive raccoon dogs  
59 held in China for fur production (20) represent 99% of the global share (Figure. S3A). However,  
60 experimental infections of these animals with SARS-CoV or SARS-CoV-2 under controlled  
61 conditions and serologic surveillance of kept or wild raccoon dogs have not been documented.

62 Since SARS-CoV and SARS-CoV-2 employ the same receptor molecule ACE2 for  
63 contact with the receptor-binding-domain (RBD) of the spike (S) protein (21), a similar range of

64 susceptible host species can be assumed. Molecular studies indicate that the ACE2 proteins of  
65 raccoon dogs can also serve as an efficient receptor for SARS-CoV (22) and SARS-CoV-2 (15).

66 Following a previously established study design (23) (Figure. 1A), we tested the  
67 susceptibility of raccoon dogs to SARS-CoV-2. Nine animals were challenged by intranasal  
68 inoculation of  $10^5$  TCID<sub>50</sub> SARS-CoV-2 2019\_nCoV Muc-IMB-1, and 3 additional animals  
69 were introduced at one day post-infection (dpi) to evaluate direct viral transmission.

## 70 **Methods**

### 71 **Study design**

72 Fourteen adult, male (n=4) and female (n=10) raccoon dogs originating from a  
73 commercial farm were used. All animals were tested negative by RT-qPCR and antibody tests  
74 (ELISA, indirect immunofluorescence assay iFAT, virus neutralization test VNT) for SARS-  
75 CoV-2 prior to the experiment. All raccoon dogs had been vaccinated against distemper, adeno-  
76 and parvovirus (Eurican® SHP, Merial, France). Animals were kept in individual stainless-steel  
77 cages (1.5m x 0.95m x 2.0m) in four separate segments at 20°C room temperature, 60-80%  
78 humidity and a 12hr/12hr (35% dimming during night modus) lighting control within a fan  
79 forced draught ventilation equipped BSL3\*\* animal facility at the Friedrich-Loeffler-Institut  
80 (FLI). Water was offered ad libitum. Animals were fed daily with 400 gr commercially produced  
81 feed for farmed foxes and raccoon dogs (Schirmer und Partner GmbH Co KG, Germany;  
82 Michael Hassel GmbH, Langenargen, Germany). The diet was supplemented with vitamins,  
83 minerals and items like one-day old chickens as described before (24). The general health status  
84 of all animals, feed uptake and defecation were recorded daily. The body weight and temperature  
85 of all animals were measured prior to inoculation and at days 2, 4, 8, 12, 16, 21, and 28 pi.

86           The outline of the experiments with an observation period of 28 days is depicted in  
87   Figure 1. Nine raccoon dogs (3 males, 6 females) were infected intranasally with  $10^5$  TCID<sub>50</sub>  
88   SARS-CoV-2 2019\_nCoV Muc-IMB-1. The inoculum of 2x1ml was administered to both  
89   nostrils using a pipette. To test viral transmission by direct contact, three naïve sentinel animals  
90   (all female) were added 24 hours post inoculation. Nasal, oropharyngeal and rectal swabs were  
91   taken at 2, 4, 8, 12, 16, 21 and 28 days post infection (dpi), blood was taken at 4, 8, 12, 16, 21  
92   and 28 dpi. Two animals each were sacrificed at day 0 (control #1, #2) day 4 (animals #1, #2),  
93   day 8 (animals #3, #4) and day 12 pi (animals #5, #6). The remaining inoculated animals  
94   (animals #7-9) and the contacts (animals #10-12) were euthanized 28 dpi. All animals were  
95   subjected to autopsy for macroscopic evaluation and tissue sampling.

96   The animal experiments were evaluated and approved by the ethics committee of the State Office  
97   of Agriculture, Food Safety, and Fishery in Mecklenburg – Western Pomerania (LALLF M-V:  
98   LVL MV/TSD/7221.3-2-010/18-12).

## 99   **Virus and cells**

100           The virus was propagated once in Vero E6 cells in a mixture of equal volumes of Eagle  
101   MEM (Hanks' balanced salts solution) and Eagle MEM (Earle's balanced salts solution)  
102   supplemented with 2mM L-Glutamine, nonessential amino acids, adjusted to 850 mg/L,  
103   NaHCO<sub>3</sub>, 120 mg/L sodium pyruvate, 10% fetal bovine serum (FBS), pH 7.2. No contaminants  
104   were detected within the virus stock preparation by metagenomic analysis employing previously  
105   published high throughput sequencing procedures Ion Torrent S5XL instrument (25, 26) and the  
106   sequence identity of the passaged virus (study accession number: PRJEB39640) was confirmed.  
107   The virus was harvested after 72 h, titrated on Vero E6 cells and stored at -80°C until further use.

## 108 **RNA extraction and detection of SARS-CoV-2**

109 Total RNA from nasal, oropharyngeal and rectal swab samples, fecal samples as well as  
110 from tissues taken at autopsy were extracted using the NucleoMagVet kit (Macherey&Nagel,  
111 Düren, Germany) according to manufacturer's instructions. Tissues were homogenized in 1 ml  
112 cell culture medium (see above) and a 5 mm steel bead in a TissueLyser (Qiagen, Hilden,  
113 Germany). Fecal samples were vortexed in sterile NaCl and the supernatant was sterile filtered  
114 (22µm) after centrifugation. Swab samples were transferred into 1 ml of serum-free tissue  
115 culture media and further processed after 30 min shaking. SARS-CoV-2 RNA was detected by  
116 an E-gene based RT-qPCR (27) using the AgPath-ID-One-Step RT-PCR kit (Thermo Fisher  
117 Scientific, Waltham, Massachusetts, USA) in a volume of 12.5 µl including 1 µl of β-Actin-  
118 mix2-HEX as internal control and 2.5 µl of extracted RNA. The reaction was performed as  
119 described before (23). Nasal swab samples from raccoon dog #2 (2 dpi) and from contact animal  
120 #10 (8 dpi) were subjected to high-throughput sequencing and compared to the inoculum (study  
121 accession number: PRJEB39640) by employing previously published high throughput  
122 sequencing procedures using Ion Torrent S5XL instrument (25, 26).

## 123 **Detection of SARS-CoV-2 reactive antibodies**

124 Serum samples collected throughout the study were tested for the presence of SARS-CoV-2  
125 reactive antibodies by indirect immunofluorescence assay (iIFA), virus neutralization test (VNT)  
126 as described before (23). For ELISA, medium-binding ELISA plates (Greiner Bio-One GmbH,  
127 Germany) were coated with SARS-CoV-2 RBD (RBD-SD1 domain, amino acids 319 – 519 of the  
128 SARS-CoV2 Spike ectodomain, for details see Appendix). The sera were diluted 1:100 in TBST  
129 and incubated on the coated and uncoated wells for 1h at room temperature followed by three

130 washes using TBST. The saliva samples were used undiluted. Reactivity was shown by adding a  
131 multi species conjugate (SBVMILK; IDvet, France) diluted 1:80 (serum) or 1:10 (saliva). After an  
132 incubation period of 1 h at room temperature, the plates were washed again and  
133 Tetramethylbenzidine (TMB) substrate (IDEXX, Switzerland) was added. The ELISA readings  
134 were taken at a wavelength of 450 nm on a Tecan Spectra Mini instrument (Tecan Group Ltd,  
135 Switzerland). The measurements were normalized to the respective samples tested on wells treated  
136 only with the coating buffer.

137 For comparison, sera were also tested in a newly developed commercial SARS-CoV-2 sVNT (28).  
138 Briefly, 1:10 serum dilutions were incubated for 30 min at 37°C with HRP-coupled RBD before  
139 transferring the samples to the capture plate pre-coated with the human ACE2 protein. After 15  
140 min incubation at 37°C, plates were washed four times. TMB substrate was added and the plate  
141 was incubated at room temperature for 15 min before stopping the reaction and reading the optical  
142 density (OD) at 450 nm. Percent inhibition was calculated as  $(1 - \text{OD sample} / \text{OD negative control})$   
143  $\times 100$ .

#### 144 **Identification of SARS-CoV-2 RBD-specific immunoglobulins**

145 SARS-CoV-2 specific immunoglobulins (Ig) were comparatively investigated in sera and saliva  
146 of raccoon dogs by ELISA using exactly the same SARS-CoV-2 RBD-SD1 antigen-coated plates,  
147 serum dilutions, washing and dilution buffers, TMB substrate, incubation periods and ELISA-  
148 Reader as described above. After the incubation of the sera or saliva and the following washing,  
149 dog-specific, horseradish-peroxidase (HRP) labelled Ig antibodies (goat- $\alpha$ -dog-IgA 1:1,000 for  
150 saliva and 1:5,000 for serum; goat- $\alpha$ -dog-IgM1 1:15,000; goat- $\alpha$ -dog-IgG, goat- $\alpha$ -dog-IgG1, goat-

151  $\alpha$ -dog-IgG2 all 1:20,000; Bethyl Laboratories INC) were added and incubated for 1h at RT.  
152 Antibodies were diluted in TBST.

### 153 **Virus titration**

154 Virus titer used for infection experiments was confirmed by titration on Vero E6 cells (Biobank  
155 Friedrich-Loeffler-Institut, catalogue N° 0929) and evaluation of CPE after 5 days. RT-qPCR  
156 positive swabs and tissue samples were titrated on Vero E6 cells as well

### 157 **Autopsy, histopathology, immunohistochemistry**

158 Full autopsy was performed on all animals under BSL3 conditions. A broad spectrum of tissues  
159 was collected and fixed in 10% neutral-buffered formalin and trimmed for paraffin embedding,  
160 including the upper and lower respiratory tract, the gastro-intestinal tract, the urinary tract, brain,  
161 and main parenchyma (see appendix for details). Tissues were embedded in paraffin, and 3  $\mu$ m  
162 sections were stained with hematoxylin and eosin for light microscopical examination. For SARS-  
163 CoV-2 antigen detection was performed as described (25). Evaluation and interpretation of  
164 pathology data were performed by a board-certified pathologist (DipLECV). The severity of  
165 lesions and the distribution of SARS-CoV-2 antigen was recorded on an ordinal scoring scale with  
166 scores 0 = no lesion/antigen, 1 = rare, affected cells/tissue <5% per slide; 2 = multifocal, 6-40 %  
167 affected; 3 = coalescing, 41-80% affected; 4 = diffuse, >80% affected.

### 168 **Statistical information**

169 All data were analyzed and visualized using GraphPad Prism Version 7.0 (GraphPad Software,  
170 San Diego, CA, USA). No statistical methods were used.

171



## 172 **Results**

173 Inoculation led to productive infection in six out of nine exposed animals. Based on the  
174 lack of viral RNA detection throughout the observation period of 28 days, we concluded that  
175 infection of animals #4, #8 and #9 failed (Figure 1, panel B). While several animals showed  
176 reduced overall activity at 4 dpi (animal #4, #5, #10), none of the exposed and contact animals  
177 showed any obvious clinical sign of infection until the termination of the experiment. In particular,  
178 neither increase in body temperature nor weight loss were observed.

179 Next, we examined the presence of viral RNA and infectious virus in nasal, oropharyngeal  
180 and rectal swab samples as well as in feces by quantitative reverse transcription PCR (RT-qPCR)  
181 and titration on Vero E6 cells. Raccoon dogs started to shed virus already at 2 dpi in nasal and  
182 oropharyngeal swabs (Figure 2, panels A, B). While infectious virus was isolated from individual  
183 animals up to 4 dpi (Figure. 2B), viral RNA was present in nasal swabs up to 16 dpi (animal #7,  
184 Figure 2, panel C). Viral genome loads were highest in nasal swabs (mean genome copies  
185 Log<sub>10</sub>/ml: 3.2, min: 1.0, max: 6.45), followed by oropharyngeal swabs (2.9; 0.54-4.39) and rectal  
186 swabs (0.71; 0.31-1.38, Figure 2, panel A). Virus titrations revealed the same trend, with the  
187 highest viral titres of up to 4.125 Log<sub>10</sub> TCID<sub>50</sub>/ml in nasal swabs at 2 dpi. Infectious virus was  
188 never isolated from rectal swabs. In general, virus isolation failed above quantification cycle (Cq)-  
189 values of around 27 (Appendix Figure 1).

190 Virus was transmitted to two of three contact animals (#10, #11) (Figure 1, panel B, Figure  
191 2, panel C). One contact raccoon dog (#12) remained negative due to the fact that both cage  
192 neighbors (#8, #9, Figure 1, panel B), did not shed virus after inoculation. In contact animals, viral  
193 RNA indicative of infection was first detected at 8 dpi (7 days post contact (dpc), #10). As in the

194 inoculated animals, excretion in contact animals was mainly via nasal secretions and lasted until  
195 16 dpi (15 dpc) and virus isolation yielded viral titers of 1.625 Log<sub>10</sub> TCID<sub>50</sub>/ml in nasal swabs  
196 of one contact animal (#10) at 8 dpi (7 dpc).

197 Tissues and body fluids of euthanized animals were tested for the presence of SARS-CoV-  
198 2 RNA and replicating virus at day 4, 8, 12, and 28 pi (Figure 2, panel D). Highest viral genome  
199 loads of up to 4.87 Log<sub>10</sub> genome copies per ml were observed in samples from the oro-nasal  
200 cavity, whereas only minute amounts were sporadically identified in other organs. The caudal,  
201 olfactory region of the oro-nasal cavity in general yielded higher viral genome loads than the  
202 cranial, respiratory region. Infectious virus could be cultivated from the nasal conchae of animals  
203 #1 (2.86 Log<sub>10</sub> TCID<sub>50</sub>/ml) and #2 (1.63 Log<sub>10</sub> TCID<sub>50</sub>/ml). Of note, none of the lung samples  
204 was positive for viral RNA, nor did any of the animals demonstrate viremia. Both animals  
205 investigated at 4 dpi had viral RNA in samples of the CNS with low genome loads (max 2.95  
206 Log<sub>10</sub> genome copies/ml), but cerebrospinal fluid was negative in all tested animals.

207 At autopsy, no gross lesions were recorded that could be assigned to the SARS-CoV-2-  
208 infection. However, histopathology identified mild rhinitis at 4, 8, and 12 dpi (animals #1-3, #5,  
209 #6). The olfactory, caudal region of the nasal cavity was more consistently affected compared to  
210 the respiratory, cranial region and included degeneration, necrosis and loss of the respiratory and  
211 olfactory epithelium, presence of intraluminal cellular debris, degeneration and necrosis of the  
212 submucosal glands, mucosal edema, endothelial swelling and acute, submucosal hemorrhage  
213 (Figure 2, panels E-G). At 4 dpi, mainly neutrophils with fewer macrophages and lymphocytes  
214 were found, later lesions showed predominantly lymphocytes and fewer neutrophils and  
215 macrophages. Mucosal coagulative necrosis with early re-epithelization and granulation tissue  
216 formation was present in one case (Figure 2, panel G, 8 dpi). At 28 dpi, one infected (#7) and one

217 contact animal (#10) showed lesions indicative for previous viral replication sites in the nasal  
218 conchae. Viral RNA was still present, but no viral antigen was found (Appendix Figure 2).

219 Immunohistochemistry verified the presence of viral antigen only in the nasal conchae.  
220 Lesion associated antigen was found to be oligofocal at day 4 (animal #1, #2) in the respiratory  
221 and olfactory epithelium and to a lesser extent at day 8 (animal #3) only in the olfactory epithelium  
222 (Figure 2, panels H-J). No viral antigen could be found at 12 dpi and 28 dpi, and neither  
223 histopathologic lesions nor viral antigen were detected in animal #4 (8 dpi) in the nasal cavity. All  
224 other tissues tested negative for SARS-CoV-2 antigen.

225 SARS-CoV-2-specific antibodies were detected in all infected animals at 8 dpi as shown  
226 by ELISA (Figure 3, panels A-G) and iFAT (> 1:64, Table 1). Titers increased up to 1:1024,  
227 detected at 28 dpi via iFAT (animal #7). Neutralizing antibodies (VNA) were observed in two of  
228 the inoculated animals (#6, #7) as early as 8 dpi (#6, 1:5.04, Tab. 1). The highest VNA titer was  
229 1:12.7 (#6, day 12; #7 day, 28). Interestingly, animal #7 showed fluctuating iFAT titers, but  
230 demonstrated a consistent increase in VNA titers until termination of the experiment (1:12.7, 28  
231 dpi). A similar pattern was observed in a surrogate assay mimicking virus neutralization (sVNT).  
232 Using the RBD of the SARS-CoV-2 spike-protein we further characterized antibody responses in  
233 an in-house ELISA (Figure 3, panels B-G, panel I). Anti-RBD IgM and IgG levels peaked at 8 and  
234 12 dpi, respectively. A similar kinetics was observed in the infected contact animals #10 and #11.  
235 RBD-specific IgG2 patterns were highly similar to those of total IgG and total RBD antibodies.  
236 IgG2 antibodies with high neutralizing capacity had also been reported in dogs and their abundance  
237 correlates with neutralizing capacity (26) (Table 1, animals #5 and 6, 8 dpi). Although the amount  
238 of IgA in serum was limited (Figure 3, panel F), a similar trend as detected for the overall serum  
239 antibody levels was observed (Figure 3, panel G), e.g. with animal #6 having the highest values,

240 and contact animals #10 and #11 reaching peak levels at later time points. RBD-specific antibodies  
241 were also detected in saliva samples 8 and 12 dpi (Figure 3, panel H-I) from animals that developed  
242 serum antibodies.

243 To test whether viral adaptations occurred during infection of raccoon dogs with this human  
244 SARS-CoV-2 isolate, we performed high throughput sequencing of SARS-CoV-2 re-isolated from  
245 nasal swabs of infected raccoon dog #2 at 2 dpi and contact animal #10 at 8 dpi yielding 100%  
246 identity to the inoculum (2019\_nCoV Muc-IMB-1).

## 247 **Discussion**

248 The present experimental study demonstrates that raccoon dogs are susceptible to SARS-  
249 CoV-2 infection and transmit the virus to contact animals. Six out of nine animals were  
250 successfully infected by intranasal inoculation. The susceptibility of raccoon dogs thus appears  
251 similar to Rousettus bats (*Rousettus aegyptiacus*) and slightly lower than ferrets (*Mustela putorius*  
252 *furo*) (23) (23). Virus shedding in nasal and oropharyngeal swabs of raccoon dogs resulted in  
253 successful onward transmission of SARS-CoV-2 to two out of three contact animals as has been  
254 observed for other animal species with direct cage neighbors (23, 29–31).

255 Increasing evidence supports the potential of several carnivore species to become infected  
256 by SARS-CoV-2 as a result of anthropo-zoonotic transmission (13), possibly leading to re-  
257 infections of humans (13). Therefore, wild carnivore species whether free-living or held in  
258 captivity should also be considered as intermediate hosts. With China's substantial contribution to  
259 the global fur production of > 50 million animals per annum (20) (Appendix Figure3, panel A), it  
260 is conceivable that raccoon dogs may have played a hitherto unexplored role in the development  
261 of the pandemic, particularly considering the very mild signs of infection, efficient replication and

262 transmission, and genetic stability. These environments with close contact between animals and  
263 an obvious interface with humans support SARS-CoV-2 transmission as was seen in several large  
264 mink farm outbreaks in The Netherlands, Denmark and Spain (13, 19, 32, 33).

265 No obvious clinical signs could be observed, which is in line with experimental studies in  
266 other carnivores, i.e. adult cats (*Felis catus*) and ferrets that showed productive SARS-CoV-2  
267 infection with no, or only mild clinical signs (23, 31). By prominent nasal virus shedding in the  
268 absence of symptoms, raccoon dogs present a picture of infection resembling asymptomatic  
269 infections in other animals reflected by restriction of virus replication to the upper respiratory  
270 tract, substantiating the role of the nasal cavity in infection as shown for other animal species (23,  
271 31), as well as the majority of human cases (34). Except for a mild rhinitis associated with the  
272 presence of viral antigen in the nasal mucosa, no other infection-related histopathological changes  
273 were observed. However, the absence of viral genome, pathohistological changes or viral antigen  
274 in the lungs of infected animals argue against raccoon dogs as a model for pulmonary manifestation  
275 of COVID-19.

276 The serological results suggest that the induction of SARS-CoV-2 specific VNA in raccoon  
277 dogs is reduced compared to ferrets but comparable to Egyptian fruit bats (23). A delayed  
278 production of VNAs cannot be excluded, but appears unlikely against the dynamic increase of the  
279 measured ELISA antibodies. A mucosal immune response to SARS-CoV-2, i.e. antibodies in  
280 saliva were detected in raccoon dogs already 12 dpi (Figure 3), supporting the use of saliva as an  
281 early and non-invasive sample for epidemiological studies (35). The limited presence of viral  
282 antigen in infected raccoon dogs at 4 dpi and the rapid decrease in viral loads prior to the  
283 development of measurable humoral immunity indicates that innate immune responses including

284 interferon, mucus movement and epithelial cell turnover may play a prominent role in reducing  
285 infection.

286 High throughput sequencing of SARS-CoV-2 re-isolated from nasal swabs of infected  
287 raccoon dogs and contact animals yielded 100% identity to the inoculum (2019\_nCoV Muc-IMB-  
288 1), demonstrating that no mutations occurred during virus replication in raccoon dogs. This is in  
289 contrast to findings in infected ferrets where two nonsynonymous single nucleotide exchanges  
290 after the ferret passage were identified (25). This may indicate that the virus is already sufficiently  
291 adapted to this putative intermediate host.

292 In conclusion, further evidence is required from research about the origin of this pandemic.  
293 Large-scale sero-epidemiological studies in susceptible animals are needed. Historical samples  
294 collected prior to the epidemic are of particular importance and should preferentially also include  
295 a time series of archived samples. Further, affected fur farms may serve as reservoirs for SARS-  
296 CoV-2 and this risk should be mitigated by efficient and continuous surveillance. While SARS-  
297 CoV-2 might be controlled in holdings by very strict measures (13, 32), a spill-over into  
298 susceptible wildlife species, in particular free living raccoon dogs representing one of the most  
299 successful invasive carnivore species in Europe (36) (Appendix Figure 3, panel B), would be even  
300 a greater challenge for elimination as long as preventive options are limited.

### 301 **Acknowledgments**

302 We acknowledge Jeannette Kliemt, Mareen Lange, Silvia Schuparis, Gabriele Czerwinski,  
303 Bianka Hillmann and Patrick Zitzow for their technical assistance and Frank Klipp, Doreen  
304 Fiedler, Harald Manthei, René Siewert, Christian Lipinski, Ralf Henkel and Dominique Lux for  
305 their support during animal experiments. Funding: Intramural funding by the German Federal

306 Ministry of Food and Agriculture was provided to the Friedrich-Loeffler-Institut. The funder of  
307 the study had no role in study design, data collection, data analysis, data interpretation, or writing  
308 of the report. T.C.M and M.B had full access to all the data in the study and had final responsibility  
309 for the decision to submit for publication.

## 310 **Disclaimers**

311 The authors declare no competing interests.

## 312 **References**

- 313 1. Tsang KW, Ho PL, Ooi GC, Yee WK, Wang T, Chan-Yeung M, et al. *A cluster of cases of severe*  
314 *acute respiratory syndrome in Hong Kong.* N Engl J Med. 2003; 348:1977–1985. doi:  
315 10.1056/NEJMoa030666. PMID: 12671062.
- 316 2. Peiris JSM, Lai ST, Poon LLM, Guan Y, Yam LYC, Lim W, et al. *Coronavirus as a possible cause of*  
317 *severe acute respiratory syndrome.* Lancet. 2003; 361:1319–1325. doi: 10.1016/s0140-6736(03)13077-2.  
318 PMID: 12711465.
- 319 3. Zaki AM, van Boheemen S, Bestebroer TM, Osterhaus ADME, Fouchier RAM. *Isolation of a novel*  
320 *coronavirus from a man with pneumonia in Saudi Arabia.* N Engl J Med. 2012; 367:1814–1820. doi:  
321 10.1056/NEJMoa1211721. PMID: 23075143.
- 322 4. Haagmans BL, Al Dhahiry SHS, Reusken CBEM, Raj VS, Galiano M, Myers R, et al. *Middle East*  
323 *respiratory syndrome coronavirus in dromedary camels: An outbreak investigation.* Lancet Infect Dis.  
324 2014; 14:140–145. doi: 10.1016/S1473-3099(13)70690-X. PMID: 24355866.
- 325 5. Drexler JF, Corman VM, Drosten C. *Ecology, evolution and classification of bat coronaviruses in the*  
326 *aftermath of SARS.* Antiviral Res. 2014; 101:45–56. doi: 10.1016/j.antiviral.2013.10.013. PMID:  
327 24184128.
- 328 6. Song H-D, Tu C-C, Zhang G-W, Wang S-Y, Zheng K, Lei L-C, et al. *Cross-host evolution of severe*  
329 *acute respiratory syndrome coronavirus in palm civet and human.* Proc Natl Acad Sci U S A. 2005;  
330 102:2430–2435. doi: 10.1073/pnas.0409608102. PMID: 15695582.
- 331 7. Reusken CB, Haagmans BL, Müller MA, Gutierrez C, Godeke G-J, Meyer B, et al. *Middle East*  
332 *respiratory syndrome coronavirus neutralising serum antibodies in dromedary camels: a comparative*  
333 *serological study.* Lancet Infect Dis. 2013; 13:859–866. doi: 10.1016/S1473-3099(13)70164-6.
- 334 8. Guan Y, Zheng BJ, He YQ, Liu XL, Zhuang ZX, Cheung CL, et al. *Isolation and characterization of*  
335 *viruses related to the SARS coronavirus from animals in southern China.* Science. 2003; 302:276–278.  
336 doi: 10.1126/science.1087139. PMID: 12958366.



- 337 9. Zhou P, Yang X-L, Wang X-G, Hu B, Zhang L, Zhang W, et al. *A pneumonia outbreak associated with*  
338 *a new coronavirus of probable bat origin*. Nature. 2020; 579:270–273. doi: 10.1038/s41586-020-2012-7.  
339 PMID: 32015507.
- 340 10. Zhang T, Wu Q, Zhang Z. *Probable Pangolin Origin of SARS-CoV-2 Associated with the COVID-19*  
341 *Outbreak*. Curr Biol. 2020; 30:1346-1351.e2. doi: 10.1016/j.cub.2020.03.022. PMID: 32197085.
- 342 11. Xiao K, Zhai J, Feng Y, Zhou N, Zhang X, Zou J-J, et al. *Isolation of SARS-CoV-2-related*  
343 *coronavirus from Malayan pangolins*. Nature. 2020; 583:286–289. doi: 10.1038/s41586-020-2313-x.  
344 PMID: 32380510.
- 345 12. Leroy EM, Ar Gouilh M, Brugère-Picoux J. *The risk of SARS-CoV-2 transmission to pets and other*  
346 *wild and domestic animals strongly mandates a one-health strategy to control the COVID-19 pandemic*.  
347 One Health. 2020:100133. doi: 10.1016/j.onehlt.2020.100133. PMID: 32363229.
- 348 13. Oreshkova N, Molenaar RJ, Vreman S, Harders F, Oude Munnink BB, Hakze-van der Honing RW, et  
349 al. *SARS-CoV-2 infection in farmed minks, the Netherlands, April and May 2020*. Euro Surveill. 2020; 25.  
350 doi: 10.2807/1560-7917.ES.2020.25.23.2001005. PMID: 32553059.
- 351 14. Andersen KG, Rambaut A, Lipkin WI, Holmes EC, Garry RF. *The proximal origin of SARS-CoV-2*.  
352 Nat Med. 2020; 26:450–452. doi: 10.1038/s41591-020-0820-9.
- 353 15. Zhai X, Sun J, Yan Z, Zhang J, Zhao J, Zhao Z, et al. *Comparison of SARS-CoV-2 spike protein*  
354 *binding to ACE2 receptors from human, pets, farm animals, and putative intermediate hosts*. J Virol.  
355 2020;JVI.00831-20. doi: 10.1128/JVI.00831-20.
- 356 16. Liu P, Jiang J-Z, Wan X-F, Hua Y, Li L, Zhou J, et al. *Are pangolins the intermediate host of the*  
357 *2019 novel coronavirus (SARS-CoV-2)?* PLoS Pathog. 2020; 16:e1008421. doi:  
358 10.1371/journal.ppat.1008421. PMID: 32407364.
- 359 17. Lam TT-Y, Jia N, Zhang Y-W, Shum MH-H, Jiang J-F, Zhu H-C, et al. *Identifying SARS-CoV-2-*  
360 *related coronaviruses in Malayan pangolins*. Nature. 2020; 583:282–285. doi: 10.1038/s41586-020-2169-  
361 0. PMID: 32218527.
- 362 18. Newman A, Smith D, Ghai RR, Wallace RM, Torchetti MK, Loiacono C, et al. *First Reported Cases*  
363 *of SARS-CoV-2 Infection in Companion Animals - New York, March-April 2020*. MMWR Morb Mortal  
364 Wkly Rep. 2020; 69:710–713. doi: 10.15585/mmwr.mm6923e3. PMID: 32525853.
- 365 19. *Promed Post – ProMED-mail*; 2020 Jul 29 [accessed 2020 Jul 29]. [https://promedmail.org/promed-](https://promedmail.org/promed-post/?id=20200717.7584560)  
366 [post/?id=20200717.7584560](https://promedmail.org/promed-post/?id=20200717.7584560).
- 367 20. ACTAsia.org. *China's fur trade and its position in the global fur industry*; 2019.  
368 <https://www.actasia.org/wp-content/uploads/2019/10/China-Fur-Report-7.4-DIGITAL-2.pdf>.
- 369 21. Hoffmann M, Kleine-Weber H, Schroeder S, Krüger N, Herrler T, Erichsen S, et al. *SARS-CoV-2 Cell*  
370 *Entry Depends on ACE2 and TMPRSS2 and Is Blocked by a Clinically Proven Protease Inhibitor*. Cell.  
371 2020; 181:271-280.e8. doi: 10.1016/j.cell.2020.02.052. PMID: 32142651.
- 372 22. Xu L, Zhang Y, Liu Y, Chen Z, Deng H, Ma Z, et al. *Angiotensin-converting enzyme 2 (ACE2) from*  
373 *raccoon dog can serve as an efficient receptor for the spike protein of severe acute respiratory syndrome*  
374 *coronavirus*. J Gen Virol. 2009; 90:2695–2703. doi: 10.1099/vir.0.013490-0.



- 375 23. Schlottau K, Rissmann M, Graaf A, Schön J, Sehl J, Wylezich C, et al. *Experimental Transmission*  
376 *Studies of SARS-CoV-2 in Fruit Bats, Ferrets, Pigs and Chickens*. SSRN. Epub ahead of print. doi:  
377 10.2139/ssrn.3578792.
- 378 24. Freuling CM, Eggerbauer E, Finke S, Kaiser C, Kaiser C, Kretzschmar A, et al. *Efficacy of the oral*  
379 *rabies virus vaccine strain SPBN GASGAS in foxes and raccoon dogs*. *Vaccine*. 2019; 37:4750–4757.  
380 doi: 10.1016/j.vaccine.2017.09.093. PMID: 29042202.
- 381 25. Wylezich C, Papa A, Beer M, Höper D. *A Versatile Sample Processing Workflow for Metagenomic*  
382 *Pathogen Detection*. *Sci Rep*. 2018; 8:13108. doi: 10.1038/s41598-018-31496-1. PMID: 30166611.
- 383 26. Wylezich C, Calvelage S, Schlottau K, Ziegler U, Pohlmann A, Höper D, et al. *Next-generation*  
384 *diagnostics: virus capture facilitates a sensitive viral diagnosis for epizootic and zoonotic pathogens*  
385 *including SARS-CoV-2*. Epub ahead of print. doi: 10.1101/2020.06.30.181446.
- 386 27. Etievant S, Bal A, Escuret V, Brengel-Pesce K, Bouscambert M, Cheynet V, et al. *Performance*  
387 *Assessment of SARS-CoV-2 PCR Assays Developed by WHO Referral Laboratories*. *J Clin Med*. 2020; 9.  
388 doi: 10.3390/jcm9061871. PMID: 32560044.
- 389 28. Tan CW, Chia WN, Chen MI-C, Hu Z, Young BE, Tan Y-J, et al. *A SARS-CoV-2 surrogate virus*  
390 *neutralization test (sVNT) based on antibody-mediated blockage of ACE2-spike (RBD) protein-protein*  
391 *interaction*. Epub ahead of print. doi: 10.21203/rs.3.rs-24574/v1.
- 392 29. Richard M, Kok A, Meulder D de, Bestebroer TM, Lamers MM, Okba NMA, et al. *SARS-CoV-2 is*  
393 *transmitted via contact and via the air between ferrets; 2020*.
- 394 30. Kim Y-I, Kim S-G, Kim S-M, Kim E-H, Park S-J, Yu K-M, et al. *Infection and Rapid Transmission*  
395 *of SARS-CoV-2 in Ferrets*. *Cell Host Microbe*. Epub ahead of print. doi: 10.1016/j.chom.2020.03.023.  
396 PMID: 32259477.
- 397 31. Shi J, Wen Z, Zhong G, Yang H, Wang C, Huang B, et al. *Susceptibility of ferrets, cats, dogs, and*  
398 *other domesticated animals to SARS-coronavirus 2*. *Science*. Epub ahead of print. doi:  
399 10.1126/science.abb7015. PMID: 32269068.
- 400 32. *Promed Post – ProMED-mail; 2020 Jul 9 [accessed 2020 Jul 9]*. [https://promedmail.org/promed-](https://promedmail.org/promed-post/?id=7533033)  
401 [post/?id=7533033](https://promedmail.org/promed-post/?id=7533033).
- 402 33. Enserink M. *Coronavirus rips through Dutch mink farms, triggering culls*. *Science*. 2020; 368:1169.  
403 doi: 10.1126/science.368.6496.1169. PMID: 32527808.
- 404 34. Wölfel R, Corman VM, Guggemos W, Seilmaier M, Zange S, Müller MA, et al. *Virological*  
405 *assessment of hospitalized patients with COVID-2019*. *Nature*. 2020; 581:465–469. doi: 10.1038/s41586-  
406 020-2196-x. PMID: 32235945.
- 407 35. Randad PR, Pisanic N, Kruczynski K, Manabe YC, Thomas D, Pekosz A, et al. *COVID-19 serology*  
408 *at population scale: SARS-CoV-2-specific antibody responses in saliva*. medRxiv.  
409 2020:2020.05.24.20112300. doi: 10.1101/2020.05.24.20112300. PMID: 32511537.
- 410 36. Kauhala K, Kowalczyk R. *Invasion of the raccoon dog *Nyctereutes procyonoides* in Europe: History*  
411 *of colonization, features behind its success, and threats to native fauna*. *Curr Zool*. 2011; 57:584–598.  
412 doi: 10.1093/czoolo/57.5.584.

413

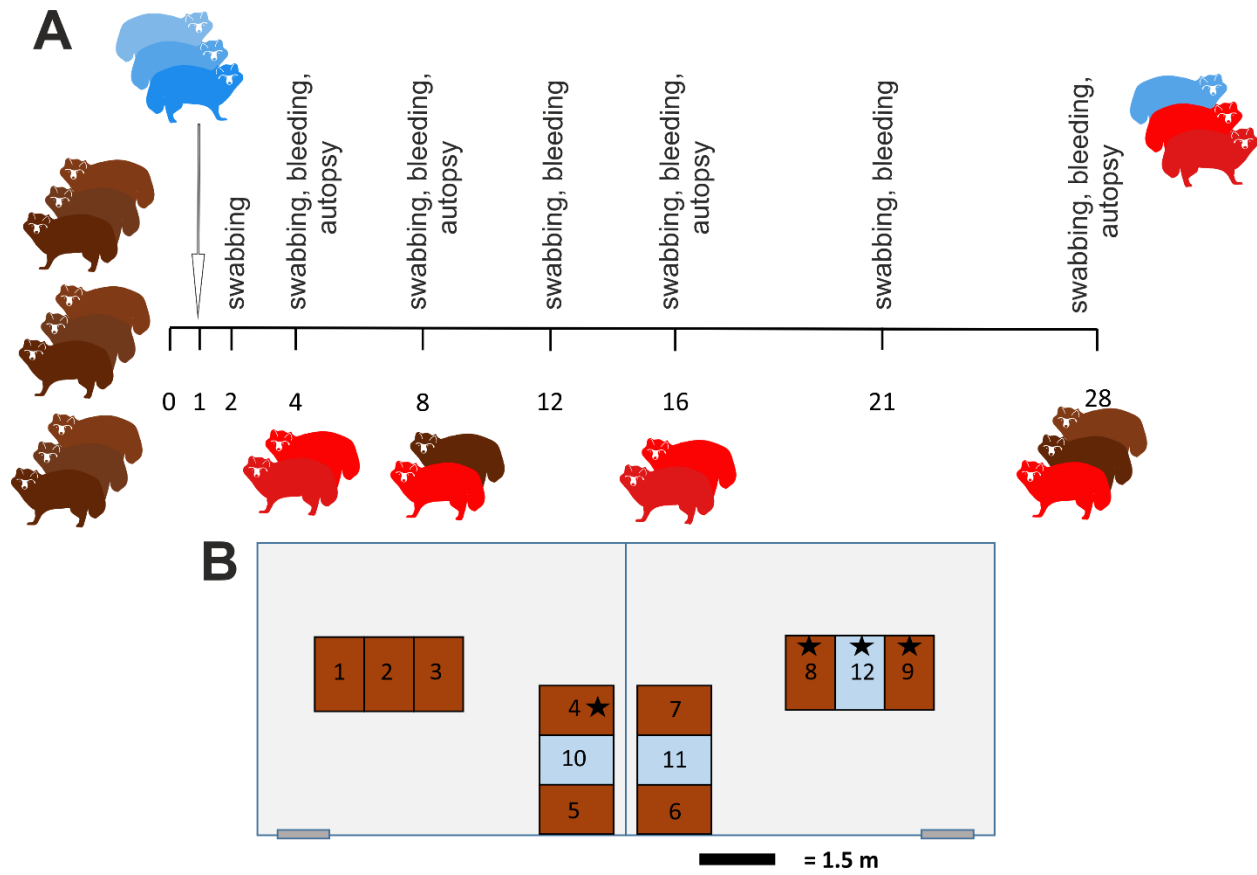
414

415 **Table 1.** Serological response of raccoon dogs to SARS-CoV-2 infection using the indirect  
 416 immunofluorescence assay (iIFA), the virus neutralization test (VNT) and a surrogate Virus  
 417 Neutralization test (sVNT). Positive results are highlighted in red (bold font) for inoculated (#1-  
 418 9) and contact (#10-12) animals. No serological response on day 0 and day 4 pi (data not shown).

No.	Day 8pi			Day 12pi			Day 16pi			Day 21pi			Day 28pi		
	iIFAT	VNT	sVNT	iIFAT	VNT	sVNT	iIFAT	VNT	sVNT	iIFAT	VNT	sVNT	iIFAT	VNT	sVNT
#1															
#2															
#3	<b>1:128</b>	< 1:4	<b>56.39</b>												
#4	< 1:20	< 1:2	13.42												
#5	<b>1:64</b>	< 1:2	<b>52.26</b>	<b>1:64</b>	< 1:2	<b>71.62</b>									
#6	<b>1:128</b>	<b>1:5.04</b>	<b>52.19</b>	<b>1:64</b>	<b>1:12.7</b>	<b>83.99</b>									
#7	<b>1:128</b>	< 1:4	<b>38.94</b>	<b>1:64</b>	< 1:2	<b>72.56</b>	<b>1:64</b>	<b>1:4</b>	<b>76.22</b>	<b>1:128</b>	<b>1:10.08</b>	<b>84.99</b>	<b>1:1024</b>	<b>1:12.7</b>	<b>88.57</b>
#8	< 1:20	< 1:2	6.62	< 1:20	< 1:2	9.20	< 1:20	< 1:2	10.58	< 1:20	< 1:2	4.99	< 1:20	< 1:2	-8.80
#9	< 1:20	< 1:2	2.12	< 1:20	< 1:2	16.08	< 1:20	< 1:2	11.42	< 1:20	< 1:2	3.99	< 1:20	< 1:2	-2.88
#10	< 1:20	< 1:2	3.02	< 1:20	< 1:2	<b>24.62</b>	<b>1:64</b>	< 1:2	<b>62.34</b>	<b>1:128</b>	< 1:4	<b>82.31</b>	<b>1:512</b>	< 1:4	<b>82.98</b>
#11	< 1:20	< 1:2	-9.55	< 1:20	< 1:2	<b>47.88</b>	<b>1:64</b>	< 1:2	<b>71.94</b>	<b>1:128</b>	<b>1:5.04</b>	<b>69.10</b>	<b>1:256</b>	< 1:4	<b>81.82</b>
#12	< 1:20	< 1:2	-0.77	< 1:20	< 1:2	8.89	< 1:20	< 1:2	12.17	< 1:20	< 1:2	<b>22.91</b>	< 1:20	< 1:2	7.34

419

420



421

422 **Figure 1.** Study design (A) Outline of the in vivo experiments with an observation period of 28

423 days. Animals (n=9) were inoculated intranasally with  $10^5$  TCID<sub>50</sub>/ml and three naïve direct

424 contacts were added 1 dpi. On day 4 (animals #1, #2), day 8 (#3, #4), and 12 (#5, #6) two

425 raccoon dogs each were sacrificed and subjected to autopsy. All remaining animals were

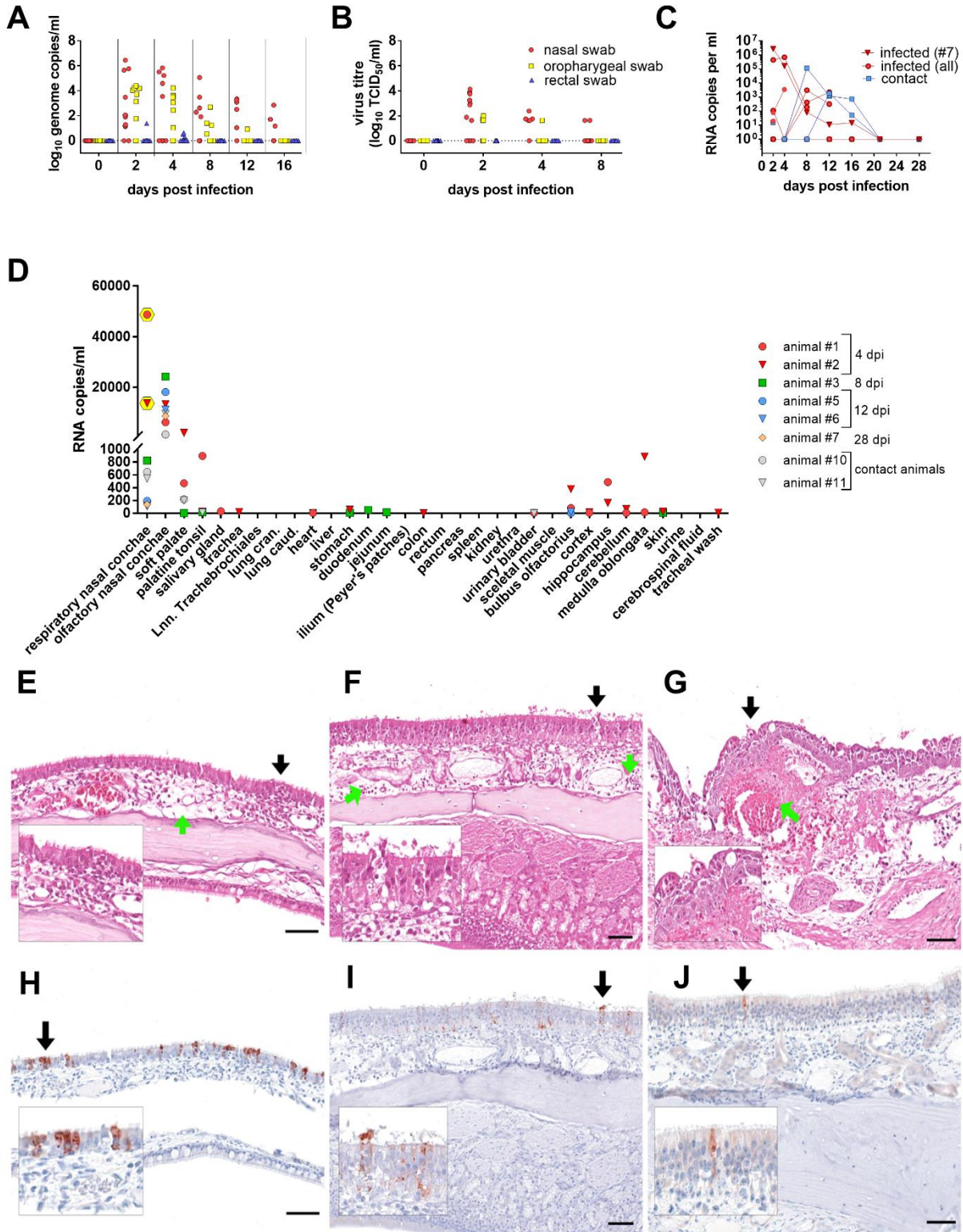
426 euthanized on day 28 pi. Animals that became infected are highlighted in red. (B) Arrangement

427 of the individual cages for the raccoon dogs in two separate rooms of the BSL 3 facility at the

428 Friedrich-Loeffler-Institut. Inoculated animals (brown), contact animals (blue) and animals that

429 remained uninfected (★) are indicated.

430

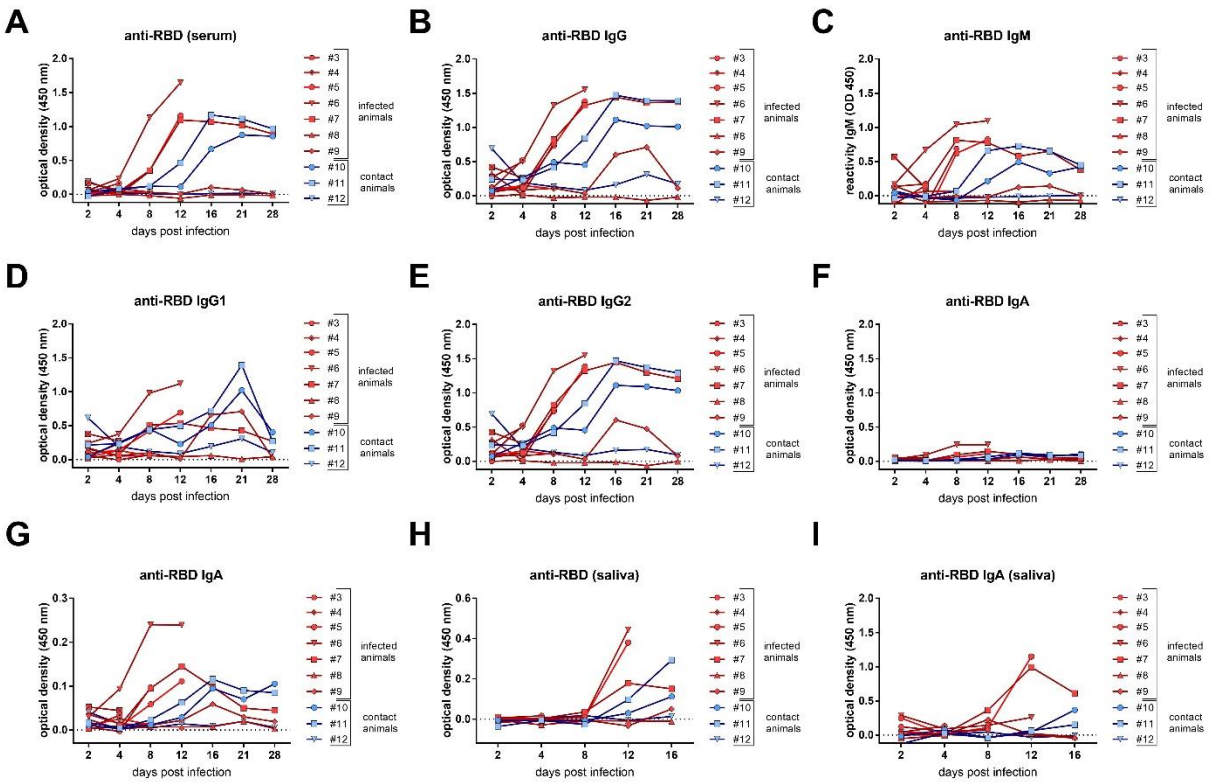


431

432 **Figure 2.** Virus detection in swab and tissue samples (A) SARS-CoV-2 viral genome loads in

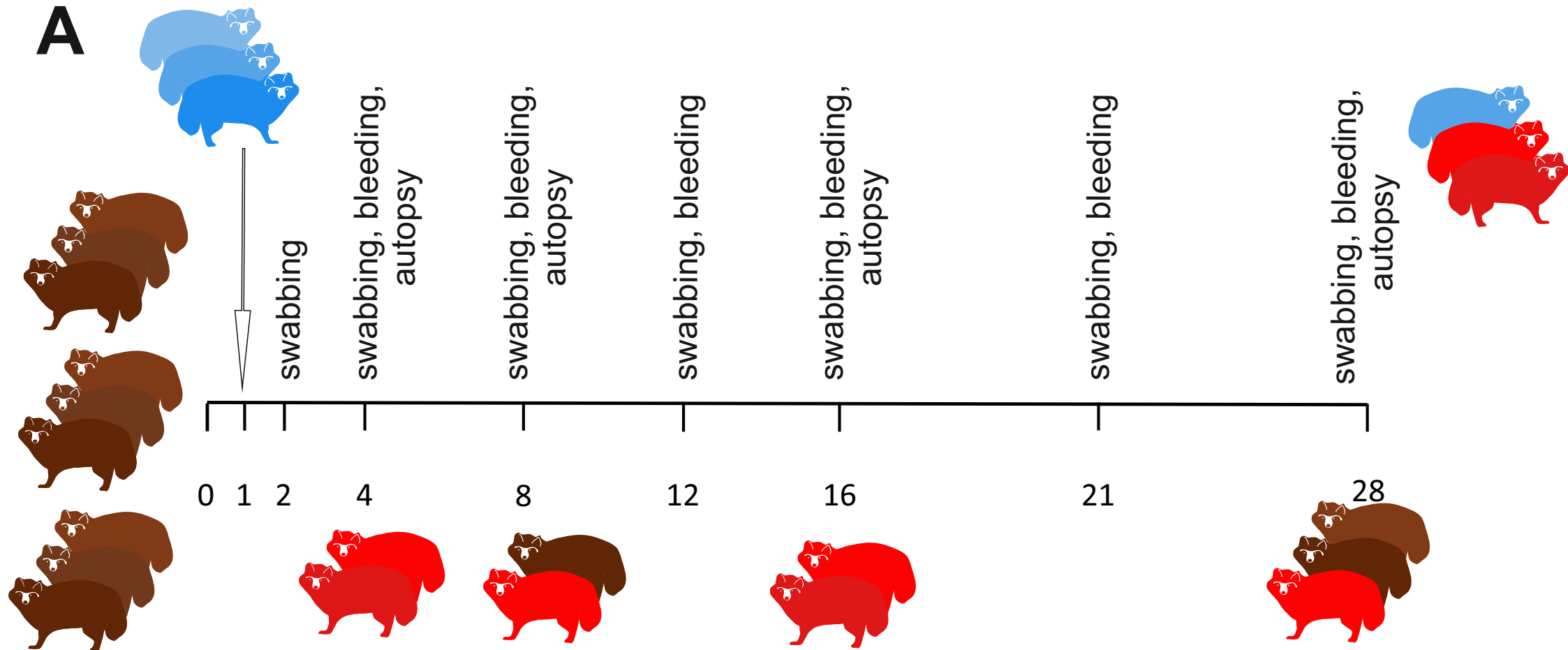
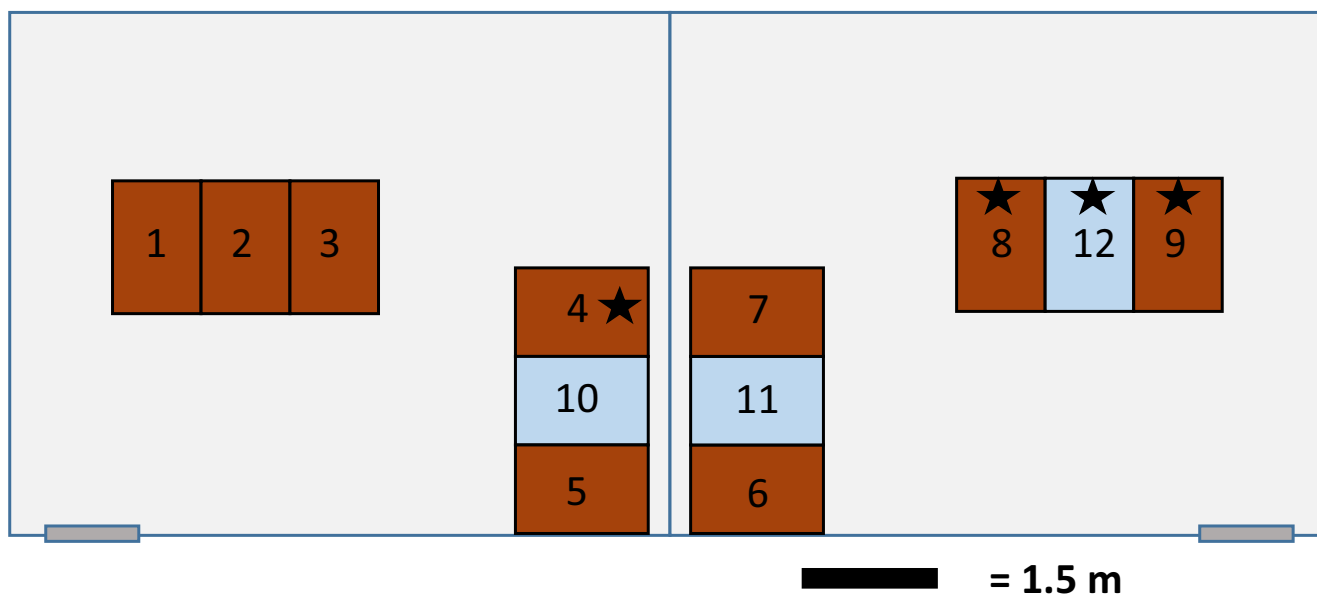
433 swab samples over time, and (B) virus titres using isolation on Vero E6 cells. Two replicates per  
434 sample were analysed and both results are shown. (C) Individual viral loads of nasal swabs taken  
435 from infected and contact animals. (D) Viral genome loads in organs, infectious virus was  
436 isolated only from nasal conchae at 4 dpi (yellow hexagons) from animal #1 (2.86 Log<sub>10</sub>  
437 TCID<sub>50</sub>/ml) and animal #2 (1.63 Log<sub>10</sub> TCID<sub>50</sub>/ml). (E) Rhinitis, respiratory region, with mucosal  
438 edema (green arrow) and epithelial degeneration with inflammation (black arrow, see also inlay)  
439 at 4 dpi. (F) Rhinitis, olfactory region, with mucosal edema and inflammation (green arrows) and  
440 epithelial necrosis and loss with minimal intraluminal debris (black arrow, see also inlay), 4 dpi.  
441 (G) Rhinitis, olfactory region, focal coagulative necrosis and hemorrhage (green arrow) and  
442 epithelial necrosis with early re-epithelisation (black arrow, see also inlay), 8 dpi. (H)  
443 Intralesional viral antigen oligofocal in the respiratory epithelium, 4 dpi, (I) Intralesional antigen  
444 labelling oligofocal in the olfactory epithelium, 4 dpi. (J) Single antigen-positive olfactory cells,  
445 8 dpi. (E-G) Histopathology, hematoxylin & eosin stain, (H-J) immunohistochemistry, ABC  
446 method, AEC chromogen (red-brown), Mayer's hematoxylin counter stain (blue). All bars = 50  
447 μm



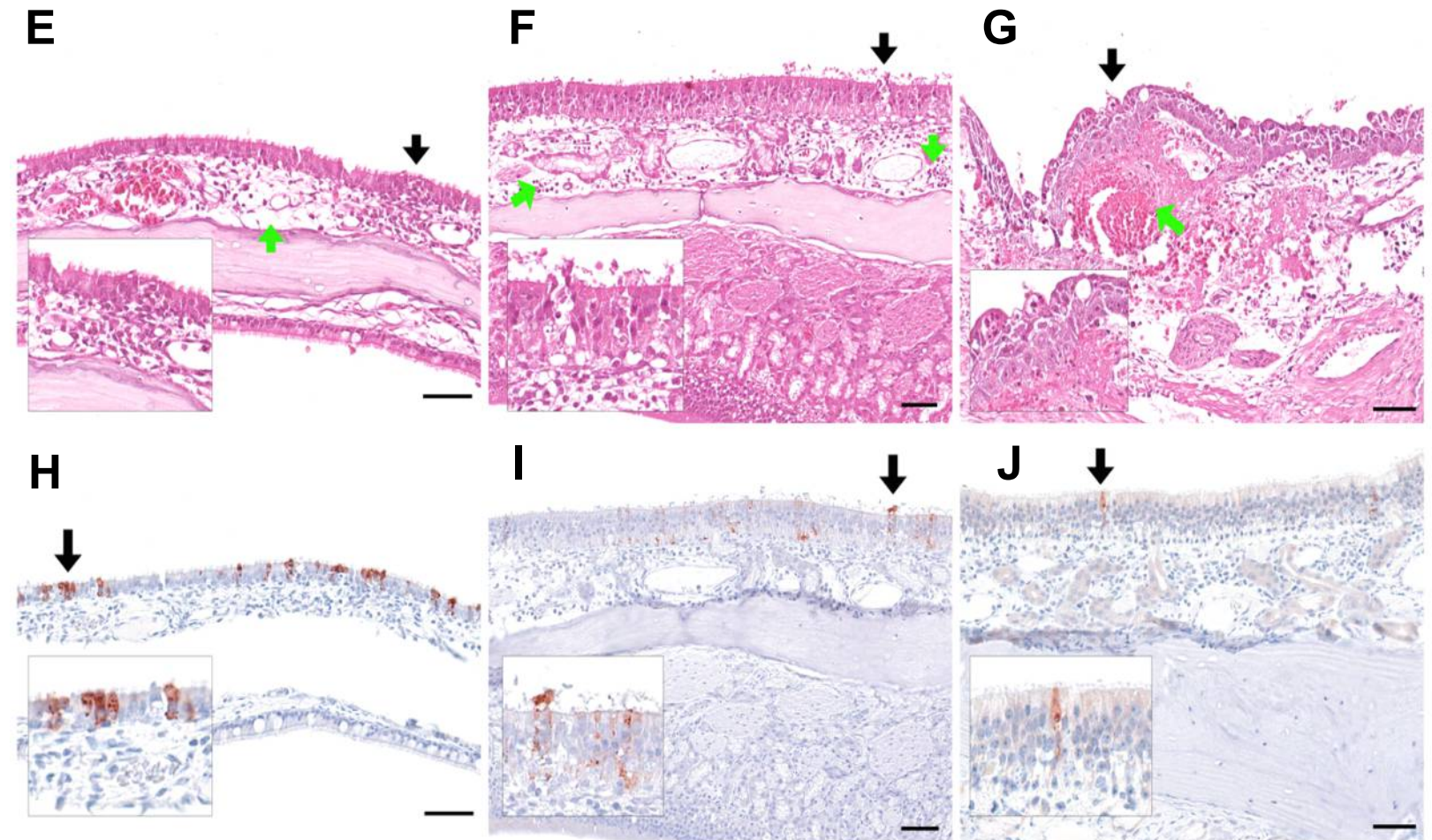
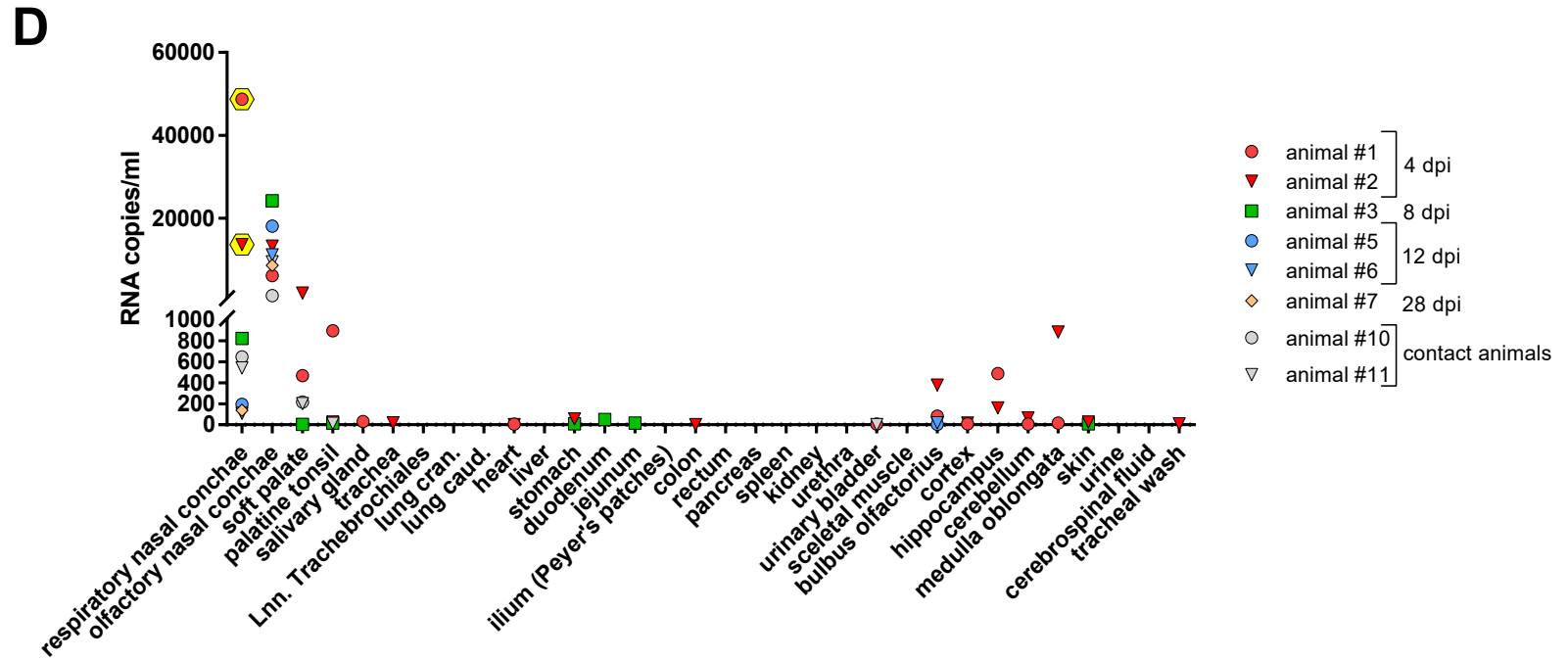
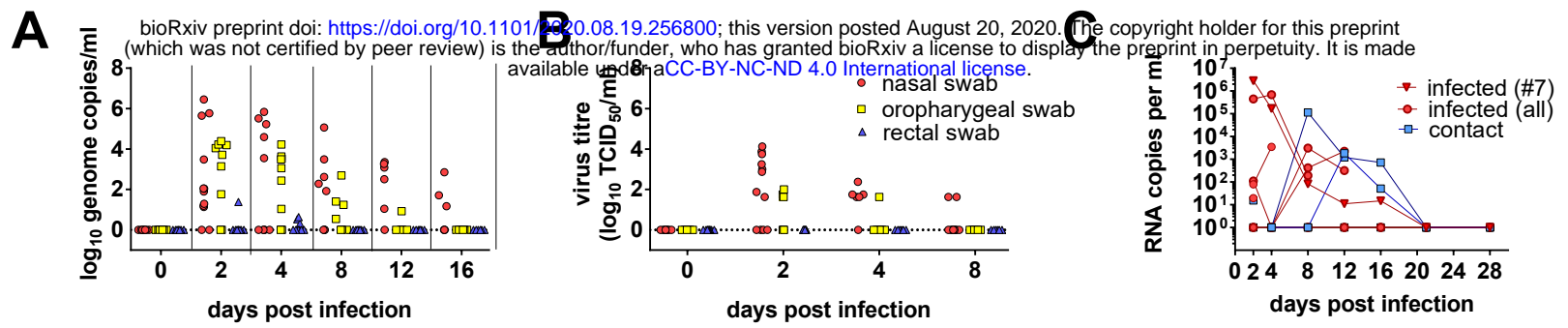


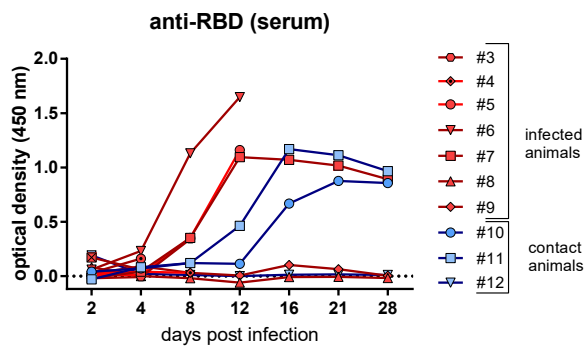
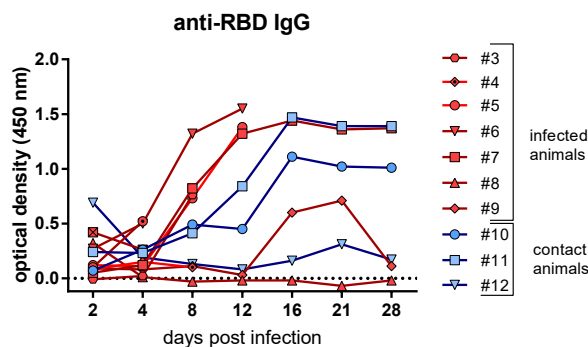
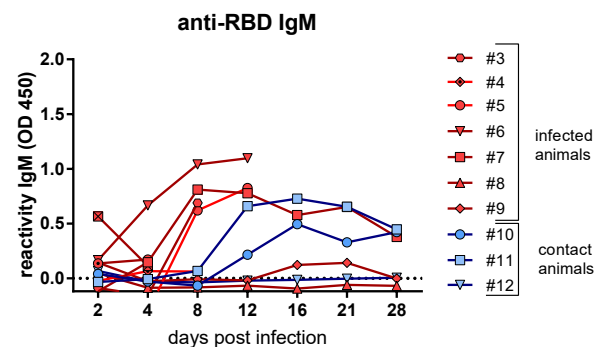
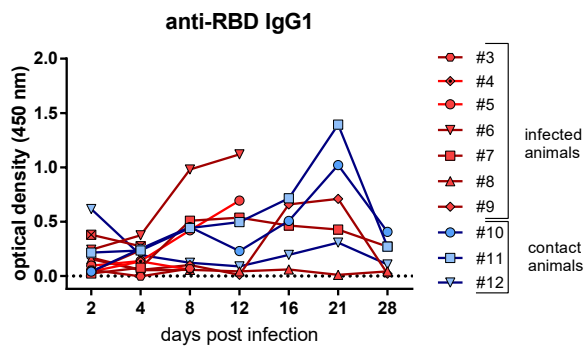
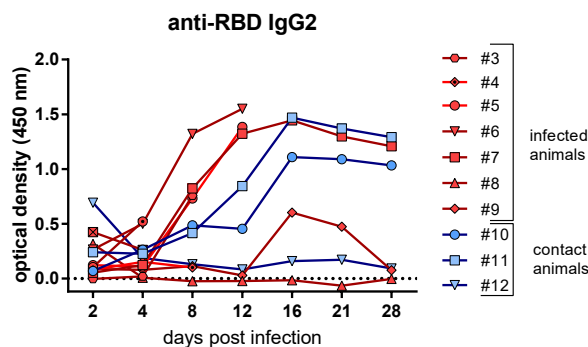
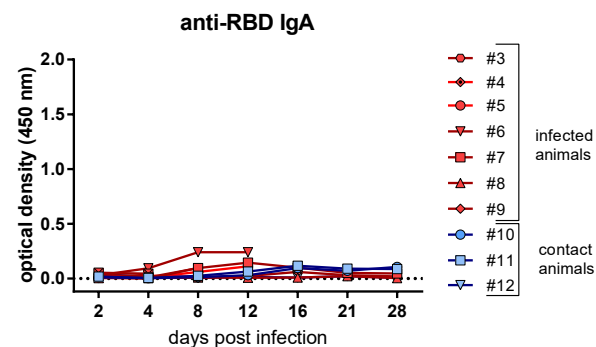
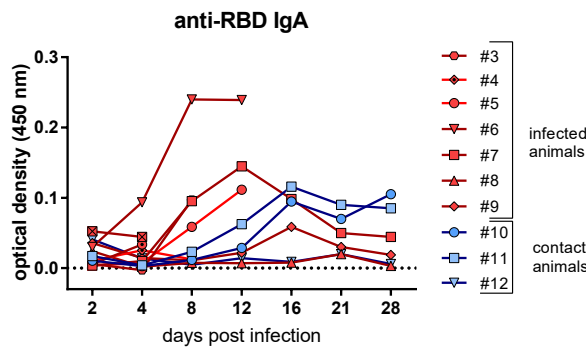
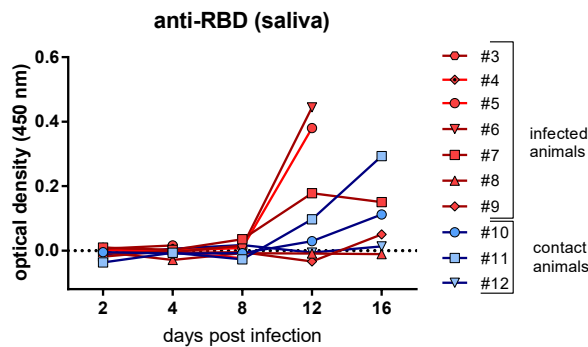
448

449 **Figure 3.** SARS-CoV-2-specific antibody response (A) Individual immune response in sera as  
450 measured using an in-house RBD ELISA with a multi species conjugate (SBVMILK, kindly  
451 provided by ID-VET, Grabels, FRANCE); (B) with a secondary anti-dog IgG-conjugate; (C)  
452 with a secondary anti-dog IgM; (D) with a secondary anti-dog IgG1; (E) with a secondary anti-  
453 dog IgG2; (F) with RBD as antigen and a secondary anti-dog IgA, at the same scale, and (G) at a  
454 zoomed scale. (H) Total anti-RBD antibodies in saliva and (I) anti-RBD IgA in saliva

**A****B**





**A****B****C****D****E****F****G****H****I**